Title

Crucial Impact of Hydrophilicity on the Self-Assembled 2D Colloidal Crystals Using Langmuir—Blodgett Method

Journal

Langmuir, 36(34)

ISSN

0743-7463

Authors

Wu, Heping
Niu, Gang
Ren, Wei
et al.

Publication Date

2020-09-01

DOI

10.1021/acs.langmuir.0c01168

Peer reviewed

LANGMUIR

pubs.acs.org/Langmuir Article

Crucial Impact of Hydrophilicity on the Self-Assembled 2D Colloidal Crystals Using Langmuir–Blodgett Method

Heping Wu, Gang Niu,* Wei Ren,* Luyue Jiang, Owen Liang, Jinyan Zhao, Yangyang Liu, and Ya-Hong Xie*

Cite This: *Langmuir* 2020, 36, 10061–10068 Read Online

ACCESS | Metrics & More | Article Recommendations | Supporting Information

ABSTRACT: Large-scale close-packed two-dimensional (2D) colloidal crystal with high coverage is indispensable for various promising applications. The Langmuir–Blodgett (LB) method is a powerful technique to prepare 2D colloidal crystals. However, the self-assembly and movement of microspheres during the whole LB process are less analyzed. In this study, we clarify the crucial impact of hydrophilicity of the microspheres on their self-assembly in the LB process and on the properties of the prepared 2D colloidal crystals. The characteristic surface pressure–area isotherms of the microspheres have been analyzed and adjusted by only counting the quantity of the microspheres on the water surface, which leads to more accurate results. The critical surface pressures for hydrophilic and hydrophobic microspheres are about 61 and 46 mN/m, respectively. The decrease of the surface hydrophilicity of microspheres facilitates their self-assembly on the water surface, which further leads to higher coverage and less defects of the 2D colloidal crystals. A coverage of as high as 97% was obtained using hydrophobic microspheres. Entropy and intersphere capillary forces drive the self-assembly and transportation of the microspheres, respectively. Caused by the diffraction of visible light, opposite contrasts at local adjacent regions on the surface of the 2D colloidal crystals have been observed. The understanding of self-assembly of the microspheres during the LB process paves the way to fabricate the high-quality 2D colloidal crystals for various applications such as photonic papers and inks, stealth materials, biomimetic coatings, and related nanostructures.

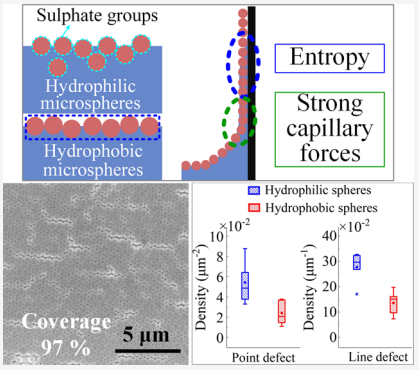

INTRODUCTION

Colloidal crystals, periodically ordered arrays of monodisperse colloidal particles (typically, micro- and nanospheres ranging from a few micrometers to tens of nanometers in diameter), represent a new class of self-assembled materials.[1] Among them, two-dimensional (2D) colloidal crystals are attracting more and more attention because of their unique optical and structural properties which have great application potentials. For example, colloidal lithography[2] based on 2D colloidal crystals is a facile, inexpensive, efficient, and flexible nanofabrication approach toward a wide variety of 2D patterned nanostructures with high controllability and reproducibility. Other important applications vary from photonics, electronics, optoelectronic devices to biological and chemical sensing, surface wetting, and energy conversion.[3,4] In these applications, the development of 2D colloidal crystals with high coverage and low defects rate is a prerequisite.

Various methods to prepare monolayer-thick colloidal crystals have been developed, which can be generally divided into five categories: drop coating, dip coating, spin coating, self-assembly at the gas–liquid interface, and electrophoretic deposition.[5,6] Among them, the first three methods are relatively easy but some of their technological parameters need to be precisely controlled, such as the evaporation rate,[7] the lifting speed of the substrate, and so forth.[8−10] Self-assembly at the gas/liquid interface[11,12] is an effective way to prepare large-scale 2D colloidal crystals, with two possible ways to transfer the 2D crystal at the interface to a solid substrate, that is, the scooping transfer method (manually)[13] and the Langmuir–Blodgett (LB) method,[14] between which the LB method is a controllable self-assembly technology having advantages like high degree of mechanization and good reproducibility.

Last decade has witnessed continuous efforts using the LB method to prepare 2D colloidal crystals, including both non-close-packed ones and the close-packed ones. Compared to the non-close-packed counterpart, the close-packed 2D colloidal crystals have less requirements of the substrates[15] as well as the material of the colloid itself.[16] The most often used colloids to prepare the close-packed colloidal crystals are silica microspheres and polystyrene (PS) microspheres. Previous reports

Received: April 22, 2020
Revised: July 29, 2020
Published: July 30, 2020

https://dx.doi.org/10.1021/acs.langmuir.0c01168
Langmuir 2020, 36, 10061–10068

focus mainly on the optimization of the deposition parameters and the experiment conditions,[17−20] the study of the optical and physical properties of the 2D colloidal crystals,[19,21] and the improvement of LB equipment.[17,22,23] A few study has been reported on the behavior of the microspheres during the whole LB process, including self-assembly on the water surface as well as the following transferring process. Furthermore, the traditional method to measure the characteristic surface pressure−area isotherms (π−A curve)[24] is not available for the microspheres for they will sink into water severely during the dispersion period. Although these are of great significance for the preparation and optimization of the close-packed 2D colloidal crystals, the understanding of them is however hindered by the difficulties to *in situ* study the colloids at a submicrometer scale at the air/subphase interface.[25]

In this study, we analyze the self-assembly phenomenon and the transferring process of the microspheres during the whole LB process by studying the compressing area of the monolayer at the air/water interface, where the quantity of the microspheres equals to those transferred to the Si wafer. Using the same method, we analyzed the surface pressure−area isotherms for the microspheres. To achieve the high coverage 2D colloidal crystal, we optimized the fabrication parameters and particularly clarified the impact of hydrophilicity of the microspheres on the coverage as well as the defects of the colloidal crystals. Furthermore, photonic properties of 2D colloidal crystals were studied.

EXPERIMENTAL SECTION

Materials. Two types of monodisperse PS latex microspheres were used, differences between which are whether the surfaces are functionalized by sulfate groups. Surface sulfated microspheres were purchased from Alfa Aesar, with a concentration of 2.5 % wt. The other type microsphere with no functional groups was purchased from Suzhou Smartynano Technology Co., Ltd, with a concentration of 5 % wt. Produced as water dispersion, both types of microspheres have a diameter of 500 nm, and the coefficient of variance is <5%. The dispersions were mixed with an equal volume of ethanol before being used. Because the microspheres were dispersed in the completely same liquid without any other additives, the differences of zeta potential between these two types of dispersions caused by the microspheres are not significant.[26] SiO_2/Si wafer (50 nm) as a substrate underwent hydrophilic treatment by immersing in a Piranha solution at 70° C for 1 h, followed by rinsing in deionized (DI) water for 3 times.

LB Assembly of 2D Colloidal Crystal. Figure 1 is a schematic illustration of the fabrication process of 2D colloidal crystals of PS microspheres using LB trough (Shanghai Zhongchen Digital Technique Apparatus Co., Ltd). Before introducing onto water in the LB trough, the mixed PS microspheres dispersion was ultrasonically treated for 30 min. The mixture was slowly dispersed on the water surface through a hydrophilic silicon wafer sheet inserted into water at an angle of 30°. The loading speed of suspended liquid was about 20 μL/min. The dispersion slowly diffused along the inclined Si wafer (shown in Figure 1a) to the air/water interface. Then, microspheres floated on the water surface and self-assembled. When more than 60% area of the water in LB trough was occupied, the sliding barrier was activated to compress the microsphere film at a speed of 0.05 mm/s. During this process, the surface pressure was measured using a Wilhelmy plate[27] (shown in Figure 1a). When the setting pressure is reached, the barrier reciprocated for 3−5 times to promote the array of the microspheres at the air/water interface. Then, the silicon wafer immersed in the water bath was slowly pulled out of water. To maintain the surface pressure of the LB film on the water, sliding barrier continued compressing. After the substrate was totally lifted out of water, the wafer with the monolayer of PS microspheres was dried in the air. The 2D PS microsphere array self-assembled at the air/water interface was transferred to the Si wafer.

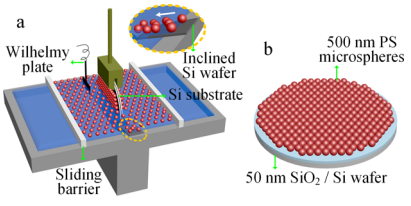

Figure 1. (a) Schematic illustration of the fabrication process of 2D colloidal crystals of PS microspheres using the LB method. (b) Schematic illustration of the 2D colloidal crystals (the defects of the 2D colloidal crystals are not shown here).

Characterization. The 2D colloidal crystals were examined using scanning electron microscopy (SEM) (FEI quanta FEG 250 and ZEISS GeminiSEM 500). Optical photographical images were acquired by a digital camera. Software Image J was used to perform the math statistics of the coverage of the 2D colloidal crystals and the crystal defects. It is noted that the coverage we used here refers to a relative coverage, which takes the coverage of a perfect close-packed array of spheres as 100%.

RESULTS AND DISCUSSION

Effect of LB Parameters. Before depositing the monolayer of the microspheres, it is necessary to study their π−A curves, where π is the surface pressure of the monolayer on the water surface, and A is the average area occupied by a single microsphere at the air/water interface. We used a mixture of 1:1 volume ratio of the aqueous dispersion and ethanol, which helps the microspheres disperse on the water surface. In dynamics, the mixing of ethanol in water largely depends on its viscosity and its compatibility with water.[28] When dripping the mixture onto water, ethanol spreads on the water surface and forms an ethanol−water bilayer. Some fraction of the alcohol evaporates, while the other fraction gradually mixes with water. At the same time, the microspheres with the drop flow on the water surface with the alcohol, forming self-assembled monolayer. When dispersing the microparticles on the water, the surface pressure of the monolayer changes with the concentration of the particles. When the density of particles increases, the area occupied by an individual particle becomes smaller, leading to a lower surface tension of water and a larger surface pressure formed by the particle monolayer. Surface pressure in the LB trough can be described by eq 1.[29]

$$\pi = \gamma_0 - \gamma_s \quad (1)$$

where γ_0 is the surface tension of pure subphase, and γ_s is the surface tension of subphase with monolayer. The subphase used here is DI water.

The wettability of a microsphere at the interface is the key factor that determines the vast majority of the interactions between the particles and the interface and amongst particles adsorbed at the interface.[30,31] The sulfate groups on the surfaces greatly enhance the hydrophilicity of the microspheres, which makes the sulfated microspheres easily sink into water. Here, we name the microspheres without any surface functional groups as hydrophobic microspheres, compared with those sulfated ones (hydrophilic microspheres). The π−A curves of the two types of PS microspheres are shown in Figure 2a, where the green curve represents the hydrophilic microspheres before adjustment, the blue and red curves represent the hydrophilic microspheres (sulfated) and the

https://dx.doi.org/10.1021/acs.langmuir.0c01168
Langmuir 2020, 36, 10061−10068

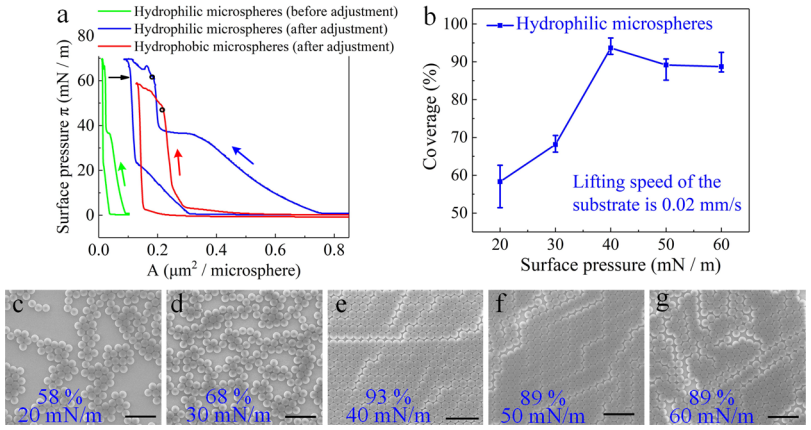

Figure 2. Depositing monolayer of 500 nm PS microspheres on silicon wafer using LB trough. (a) π–A curves of the two types of PS microspheres. For hydrophilic microspheres, the figures before (green curve) and after adjustment (blue curve) are shown. (b) Coverage of 2D colloidal crystals on the Si substrate prepared at different surface pressures using hydrophilic PS microspheres. (c–g) SEM images of the 2D colloidal crystals of hydrophilic microspheres prepared by LB method, with surface pressures of 20, 30, 40, 50, and 60 mN/m, respectively. Scale bars in the images are 2 μm.

hydrophobic ones (nonfunctionalized) after adjustment, respectively. To accomplish the measurement of the complete π–A curves, the volume of the mixtures adding onto water is 3000 μL for hydrophilic spheres and 200 μL for the hydrophobic microspheres. The number of hydrophilic and hydrophobic microspheres added onto water is 5.457×10^{11} and 7.276×10^{10}, respectively. The PS material has slight hydrophilicity with a contact angle with water of 86 ± 2°.[32] When using the traditional method to calculate the value of A (green curve in Figure 2a), all the microspheres added into water were included, which leads to an inaccuracy because a large amount of microspheres sink into water even with the utilization of the ethanol mixture. Here, we minimize this error by calculating the quantity of microspheres which are at the air/water interface. The compressing area on the water surface by the sliding barriers during the lifting period is the key parameter, which will be discussed in Figure 3a,b in detail. Comparing the green and blue curves in Figure 2a, it can be seen that at the same value of π, the corresponding A in the green curve is much lower than that in the blue curve, from which the fraction of sunk microspheres for hydrophilic ones can be calculated as high as 88%, and for hydrophobic ones is 39%. Comparing the blue and red curves, it can be seen that the two curves have rather different shapes. For hydrophobic microspheres (the red curve), the surface pressure π shows an obvious hysteresis in the regime of A = 0.13–0.30 μm^2/microsphere. The critical π of the hydrophobic microspheres is about 46 mN/m. For the hydrophilic microspheres (blue curve), the curve also shows an obvious hysteresis but in the regime of A = 0.08–0.75 μm^2/microsphere and displays a more complex feature. Starting at 0.75 μm^2/microsphere, the A decreases, and the surface pressure largely increases and reaches the critical value of ~61 mN/m.

In order to further understand the characteristic and to clarify the possible underlying mechanism, detailed SEM measurements were carried out on the samples with hydrophilic microspheres (blue curve) at the different surface pressures. Figure 2b plots the coverage variation of 2D colloidal crystals on the Si wafer fabricated via the LB method using hydrophilic microspheres as a function of the surface pressure. A lower lifting speed is good for higher coverage of the 2D colloidal crystal.[33] It is noted here that the lifting speed

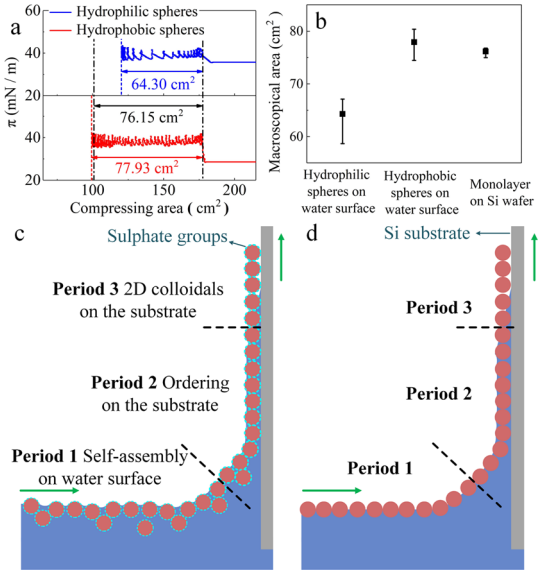

Figure 3. Self-assembly of PS microspheres on the water surface. (a) Macroscopic relationship between surface pressure and the microspheres area on the water surface during the lifting film process. The compressing area for hydrophilic microspheres is 64.30 cm^2 and for hydrophobic microspheres is 77.93 cm^2, and the area for 2D colloidal crystals on the Si substrate is 76.15 cm^2. (b) Statistics of the macroscopic area of monolayers on the Si wafer and the compressing area during the lifting process. (c) LB process of the microspheres with sulfate groups (hydrophilic). (d) LB process of the microspheres without any surface functional groups (hydrophobic).

of the substrate was fixed at 0.02 mm/s, which is the minimum value of equipment. It can be clearly seen that the coverage reaches a maximum of ~93% at the π of 40 mN/m and decreases to 89% at the π of 50 mN/m and then stays same at π of 60 mN/m. Figure 2c–g shows the surface morphology of 2D colloidal crystals shown in Figure 2b which are fabricated at different surface pressures of 20, 30, 40, 50, and 60 mN/m, respectively. The coverage of microspheres in Figures 2c–g was estimated in more detail using the Image J software. For all surface pressures, five regions with 33 × 25 μm^2 square were analyzed.

https://dx.doi.org/10.1021/acs.langmuir.0c01168
Langmuir 2020, 36, 10061–10068

Impact of Hydrophilicity of Microspheres on Self-Assembly. Considering that the hydrophilicity of microspheres impacts their self-assembly on the water surface as well as the coverage of the 2D colloidal crystals on the Si substrates, we therefore studied the differences between microspheres with sulfated surfaces (hydrophilic) and without any surface functional groups (hydrophobic). We note here that the compressing area rather than the average area of a single microsphere (i.e., A in the green curve shown in Figure 2a) was crucial during the lifting process. It is because the area needs to be limited at the air/water interface for the study of self-assembly, whereas average area A before adjustment represents all the microspheres added into water including those sunk into water. According to the experiment observations, the microspheres at the air/water interface would stay close-packed and transfer to the substrate instead of sinking into water during the compressing process.

2D colloidal crystals composed of microspheres with the sulfated surface (hydrophilic) and pure surface (hydrophobic) were prepared with same fabrication parameters with a lifting speed of 0.02 mm/s and a surface pressure of 40 mN/m. Figure 3a shows the variation of the surface pressure (π) as a function of the monolayer area of microspheres on the water surface during the lifting film process for hydrophilic (blue curve) and hydrophobic (red curve) microspheres. Figure 3b shows the statistics of the macroscopic area of monolayers on the Si wafer and the compressing area during the lifting process. The extracted compressing area for hydrophilic and hydrophobic microspheres are 64.30 and 77.93 cm^2, respectively. The distance (76.15 cm^2) between the two black vertical lines in Figure 3a shows the area of the 2D colloidal crystals on the Si substrate. Table 1 shows the coverage and average area of a single microsphere for two types of colloidal crystals. According to the calculation, a microsphere with 500 nm in diameter occupies 0.2165 μm^2 for ideal 2D colloidal crystals. The average area of a single microsphere on the water surface for hydrophilic microspheres (0.2031 μm^2) is lower than that for the ideal crystal, which indicated the possible existence of overlapping of the microspheres at the air/water interface. For hydrophobic microspheres, the average area occupied by a single microsphere at the air/water interface (0.2284 μm^2) is slightly larger than that on a Si wafer, indicating the good self-assembly on the water surface. This agrees well with the experimental observation for microsphere films. It can also be seen that the 2D colloidal crystals composed of hydrophobic microspheres have a coverage of 97% with the average area of a single microsphere of 0.2232 μm^2, which is close to the ideal crystals. However, for crystals composed of hydrophilic microspheres, the coverage is 93%, and the average area of a single microsphere increases to 0.2328 μm^2, which is much larger than that of the ideal crystals. It should be noted that the direct impact of the functional group ($PS-SO_4^-$) is not significant because it is at the atomic scale.[34] On the contrary, the effect of the change of hydrophilicity caused by the sulfate group is important.

Table 1. Average Area of Single Microsphere for Colloidal Crystals with Different Coverage

	average area of single sphere on water surface (μm^2)	average area of single sphere on Si wafer (μm^2)	coverage (%)
hydrophilic spheres monolayer	0.2031	0.2328	93
hydrophobic spheres monolayer	0.2284	0.2232	97
ideal 2D crystal	0.2165	0.2165	100

Above observations could certainly facilitate the understanding of the self-assembly behavior of microspheres. In fact, the whole LB process can be divided into three periods according to the position as well as the order degree of the PS microspheres, as schematically shown in Figure 3c,d for hydrophilic and hydrophobic microspheres, respectively. In period 1, the microspheres self-assemble on the water surface; in period 2, the microspheres transfer to the substrate and become ordered on the Si substrate; and in period 3, the water on the substrate evaporates and leaves the ordered colloidal crystals.

In period 1, the PS microspheres could be taken as hard spheres (HS), which have already been widely used in statistical mechanics because of their phase behavior and the importance of packing effects in many systems.[35] The force of the PS microspheres on the water surface is mainly the short-range repulsion.[36,37] In the crystallization process, the system tends to minimize its Helmholtz free energy $F = U - TS$, where U is the potential energy of the system, T is the temperature, and S is the entropy. Because HS have no potential energy, the crystallization and other phase behavior are determined entirely by entropy.[38,39] The configurational entropy of HS is decreased when they form a crystal lattice. This reduction of entropy is, however, more than compensated by an increase of entropy because of the larger free volume for local movements in the crystal lattice; space is used more efficiently in the crystal than in the disordered state. The result is that the entropy for the crystal is larger than that for the disordered state. The crystallization of the 2D colloidal crystal on the water surface depends on the volume fraction of the HS, which is controlled by the surface pressure π here. When π is higher enough, the fluid phase will transfer to a crystal phase, which could be verified by the diffraction of the visible light on the water surface. The final 2D colloidal crystal transferred to the Si wafer is greatly affected by the monolayer quality on the water surface. The 2D colloidal crystal with high coverage was obtained when π was over 40 mN/m, as shown in Figure 2e.

In spite of the crystal monolayer can be obtained on the water surface obeying the thermodynamics law, the monolayer of the two types of PS microspheres are not totally the same owing to their respective hydrophilicities. After being dispersed on the water surface, the microspheres are mainly affected by two types of forces: capillary attraction and dipolar repulsion.[40] The self-assembly happens at the balance between these two type of forces, and the equilibrium of the center-to-center separation between the spheres r_{eq} can be given as[36]

$$r_{eq} \approx \left(\varepsilon_0 \gamma \frac{a_w^{\,8}}{P^2} 768\, \pi^2 \frac{\varepsilon_{water}^{\,2}}{\varepsilon_{air}} \right)^{1/3} \tag{2}$$

where γ is the interfacial energy; a_w is radius of the water-wetted area of the sphere, which is determined by the equilibrium contact angle θ, through $a_w = a \sin\theta$; ε_{air}, ε_{water}, and ε_0 are dielectric constants of air, water, and vacuum, respectively; and P is the total electric dipole moment of the sphere which depends mainly on the surface charge density of the spheres.[36] The surface charge is affected by the surface chemistry.

https://dx.doi.org/10.1021/acs.langmuir.0c01168
Langmuir 2020, 36, 10061−10068

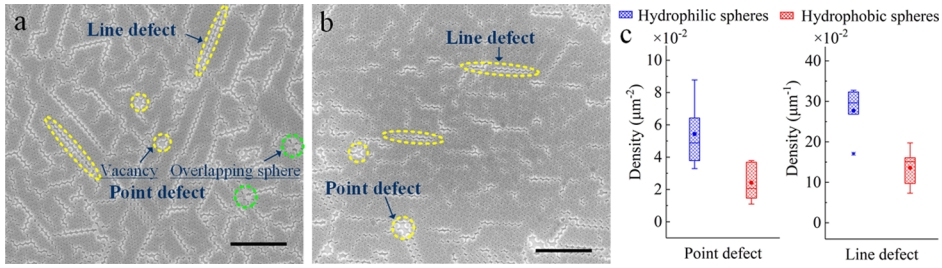

Figure 4. SEM images of the prepared 2D colloidal crystals with defects. (a) Hydrophilic microsphere crystal. (b) Hydrophobic microsphere crystal. (c) Statistics of the defects of the two types of colloidal crystals. Scale bars are 5 μm.

For hydrophilic microspheres, on the one hand, a_w is lower than that of hydrophobic microspheres. On the other hand, owing to the more surface charge generated by dissociation of surface ionizable groups, P for hydrophilic microspheres is higher than hydrophobic ones. These two effects lead to a smaller r_{eq} for hydrophilic microspheres. Compared with the hydrophobic microspheres, hydrophilic microspheres (Figure 3c) reside more in water than in air[41] and are easier to sink into the water during the dispersion process. This forms multilayers near the air/water interface and reduces the average area of single spheres. The hydrophobic microspheres (Figure 3d) own a larger r_{eq} than hydrophilic microspheres and tend to form a single layer of microspheres on the water surface, leading to the average area occupied by a single microsphere of which is slightly larger than that of ideal 2D crystals on the Si wafer.

In period 2, the microspheres move to the Si substrate then become ordered, and strong capillary forces play a crucial role in the transportation of the microspheres from the water surface to the substrate surface. It is worth noting that the capillary forces between microspheres immersed in a liquid layer on the solid substrate are many orders of magnitude larger than the capillary forces between similar particles floating attached to a single interface.[42,43] When the microspheres move toward the Si substrate via the "arc" of the liquid, the arrangement of the microspheres is still consistent with that on the water surface. With the decrease in thickness of the water layer (especially when reaching the diameter of the microspheres) on the Si wafer, the intersphere capillary forces caused by the meniscus of water surface turns out to be attractive and long-ranged. When the microspheres were transferred to the substrate, the attractive capillary force is upward while gravity of the microsphere is downward. When the upward force is larger than the downward one, the capillary force caused by the meniscus attracts the microspheres and drives them to the substrate.[37,44] The hydrophilic substrate keeps water on its surface, and it is crucial to form this meniscus of water surface between microspheres, which makes a hydrophilic substrate in most cases a prerequisite when depositing colloidal crystals using the LB method. This is the main reason why the hydrophilic SiO_2/Si substrate was chosen, the same as in many other studies of fabrication of colloidal crystals using the LB method.[21,22,33,45,46] Moreover, Si wafers are the most commonly used substrates in the microelectronic industry, which provide a large-scale and flat surface for the 2D colloidal crystal. The semiconductor technology compatibility of Si wafers is also good for the following processes such as colloidal lithography.

The array formation on the Si substrate follows a two-stage mechanism.[37] At the first stage, a "nucleus" of ordered phase appears when the first batch of microspheres arrive at the border of the wetted area on Si wafers. The microspheres are pressed to the substrate by the perpendicular component of the capillary forces there. After the nucleus formation, the following microspheres are captured by the local sucking capillary pressure pointed to the ordered array. During these two-stage processes, the order of the array is still driven by entropy. The substrate lifting up with the concentration of the microspheres near the sucking capillary forces region supplement by the compression of the sliding barrier. Such a reordering process leads to the eventual coverage of 93% and an increase of average area of a single hydrophilic microsphere, although it arranges more disorderly on the water surface. In period 3, the crystals are completely in order, and the deposited microspheres become stable with the water among the microspheres evaporating.

Impact of Hydrophilicity of Microspheres on the Defects of 2D Colloidal Crystals. In order to examine the quality of the 2D crystals formed using two types of microspheres, SEMs were performed on hydrophilic and hydrophobic microspheres samples, and the results are shown in Figure 4a,b, respectively. It can be seen that point and line defects exist in both 2D crystals. Line defects are caused by the contraction of the colloidal crystals as water evaporates thoroughly.[47] Point defects include vacancies (yellow circles) and overlapping spheres (green circles). In order to examine the defect density, five regions of two types of 2D colloidal crystal with 33 × 25 μm^2 square were analyzed. Figure 4c shows the statistic results in which blue squares represent the defects of 2D crystals of hydrophilic microspheres, and the red squares represent the hydrophobic microspheres. In the box plot, data in the box represent the plotted values from 25 to 75%, and the solid dot is the mean value. It can be seen that the average densities of point and line defects for hydrophilic microsphere crystals are about 5.4 × 10^{-2} μm^{-2} and 27.7 × 10^{-2} μm^{-1}, respectively. These densities are all much higher than those of hydrophobic microsphere crystals, which are 2.4 × 10^{-2} μm^{-2} and 13.6 × 10^{-2} μm^{-1}, respectively. Table 2

Table 2. Statistics of the 2 Types of Point Defects in the Counted Area (4125 μm^2)

	number of vacancies	number of overlapping spheres	vacancy percentage	overlapping sphere percentage
hydrophilic spheres monolayer	201	19	91.4%	8.6%
hydrophobic spheres monolayer	99	0	1	0

https://dx.doi.org/10.1021/acs.langmuir.0c01168
Langmuir 2020, 36, 10061−10068

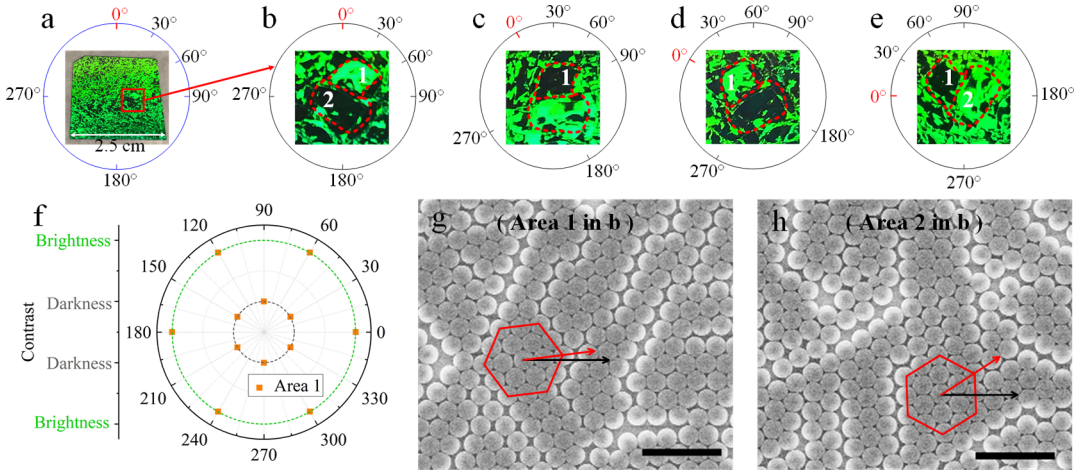

Figure 5. (a) Visible light diffraction phenomenon of the 2D colloidal crystals under white light. (b–e) Contrast of the local adjacent regions varies with the orientation of the sample. (f) Polar plot of the contrast variation of area 1 in (b–e). (g,h) SEM images of the adjacent regions [region 1 and region 2 in (b–e), respectively] at the same polarization angle. The black arrows in (g,h) are the projection of the incident light, and scale bars are 2 μm.

summarizes the statistical results of point defects (vacancies and overlapping spheres) in the 4125 μm^2 area. In the analyzed area, the point defects in hydrophilic microsphere 2D colloidal crystal are composed of 201 vacancies and 19 overlapping sphere defects, and there are only 100 vacancies in the hydrophobic counterpart. The percentage of overlapping spheres in hydrophilic microsphere crystal is 8.6%, whereas this percentage is 0% (shown in Table 2) for the hydrophobic microsphere crystal. Based on these results, it can be summarized that hydrophobic microsphere crystals have higher quality than hydrophilic ones, including higher coverage and less defects. This is due to the self-assembly process on the water surface and the ordering process transferred to the Si substrate of hydrophobic microsphere crystals. The hydrophobic microsphere monolayer transfers to the Si substrate with the good order being maintained. In contrast, for hydrophilic microspheres, the self-assembly is worse on the water surface with microspheres immersed into water, although the ordering process enhances the final crystal quality on the Si wafer.

Photonic Properties of 2D Colloidal Crystals. The photonic properties of fabricated 2D colloidal crystals are of significance. Methods commonly used to fabricate photonic crystals include the microchannel plate method, photolithography, and electron beam lithography, as well as reactive ion etching and the electrochemical methods.[48] Compared with these methods, the LB method is simpler and more inexpensive, with great potential to fabricate wafer-scale photonic crystals. Owing to the periodic structures, the 2D colloidal crystals can generate iridescent colors of structural origin based on the Bragg diffraction of light because of their complete manipulation of the propagation of light.[49,50] Such structural color can also reveal whether the structure of the 2D crystal is a long-range order. In this scenario, the diffraction light exhibits to be green, as shown in Figure 5a. The adjacent regions (marked by the red square in Figure 5a) exhibit different contrasts, which would make it suspicious that the dark region have no 2D colloidal crystal structure at all. However, this contrasts located in adjacent regions are also generated from the polarization angle of the samples, as shown in Figure 5b–e, where region 1 and region 2 show opposite brightness, and it also changes with the sample orientation. Figure 5f is the polar plot of the contrast variation of area 1 shown in Figures 5b–e. The polarization angle of each area to totally change its contrast is 60°, which equals to half of the axial angle of the 2D hexagonal close-packed (hcp) lattice. Figure 5g,h is the SEM image of the adjacent bright and dark regions in Figure 5b–e, region 1 and region 2, respectively. It can be found that the orientations of the colloidal crystals in these two regions are different, resulting in the different strength of the diffraction lights. Therefore, at the bright and dark regions, the structures of the 2D colloidal crystals both exist. The visible light scattering of colloidal crystals can be used for many applications, such as photonic papers and inks,[51] stealth materials,[52] and biomimetic coatings.[53]

CONCLUSIONS

In conclusion, high coverage and high-quality 2D colloidal crystals have been successfully fabricated on Si wafers, and the significant impact of the hydrophilicity of microspheres on their self-assembly and subsequently on 2D colloidal crystals quality have been studied. The π–A curves of hydrophilic and hydrophobic microspheres were analyzed and compared. The critical surface pressures for hydrophilic and hydrophobic microspheres are about 61 and 46 mN/m, respectively. The whole LB process was analyzed using the compressing area of the monolayer and discussed with three periods. At the air/water interface, hydrophilic microspheres tend to form multilayers. Strong intersphere capillary forces lead to the transportation of the microspheres from the water surface to the Si substrate, then on the Si wafer, the order of PS microspheres is driven by entropy as well as on the water surface. The coverage of 2D colloidal crystals composed of hydrophilic and hydrophobic microspheres is 93 and 97%, respectively. Moreover, the 2D colloidal crystal diffracts visible light, causing the different contrasts at local adjacent regions, which is in accordance with the hcp lattice. The understanding of the impact of hydrophilicity and the properties of close-packed 2D colloidal crystals using the LB method can certainly facilitate the fabrication of high-quality 2D colloidal crystals for different applications like photonic papers and inks, stealth materials, biomimetic coatings, and related nanostructures.

https://dx.doi.org/10.1021/acs.langmuir.0c01168
Langmuir 2020, 36, 10061–10068

■ ASSOCIATED CONTENT

Supporting Information

The Supporting Information is available free of charge at https://pubs.acs.org/doi/10.1021/acs.langmuir.0c01168.

Equation for calculation of the average area of single microsphere on the water surface, photographs for comparison of the relative hydrophilicity of the two types of microspheres, and AFM figures of the 2D colloidal crystals (PDF)

■ AUTHOR INFORMATION

Corresponding Authors

Gang Niu − *Electronic Materials Research Laboratory, Key Laboratory of the Ministry of Education & International Center for Dielectric Research, School of Electronic Science and Engineering, Xi'an Jiaotong University, Xi'an 710049, China;* orcid.org/0000-0002-8813-8885; Email: gangniu@xjtu.edu.cn

Wei Ren − *Electronic Materials Research Laboratory, Key Laboratory of the Ministry of Education & International Center for Dielectric Research, School of Electronic Science and Engineering, Xi'an Jiaotong University, Xi'an 710049, China;* Email: wren@mail.xjtu.edu.cn

Ya-Hong Xie − *Department of Materials Science and Engineering, University of California, Los Angeles, Los Angeles, California 90095, United States;* Email: yhx@ucla.com

Authors

Heping Wu − *Electronic Materials Research Laboratory, Key Laboratory of the Ministry of Education & International Center for Dielectric Research, School of Electronic Science and Engineering, Xi'an Jiaotong University, Xi'an 710049, China;* orcid.org/0000-0002-8587-4035

Luyue Jiang − *Electronic Materials Research Laboratory, Key Laboratory of the Ministry of Education & International Center for Dielectric Research, School of Electronic Science and Engineering, Xi'an Jiaotong University, Xi'an 710049, China*

Owen Liang − *Department of Materials Science and Engineering, University of California, Los Angeles, Los Angeles, California 90095, United States*

Jinyan Zhao − *Electronic Materials Research Laboratory, Key Laboratory of the Ministry of Education & International Center for Dielectric Research, School of Electronic Science and Engineering, Xi'an Jiaotong University, Xi'an 710049, China*

Yangyang Liu − *Electronic Materials Research Laboratory, Key Laboratory of the Ministry of Education & International Center for Dielectric Research, School of Electronic Science and Engineering, Xi'an Jiaotong University, Xi'an 710049, China*

Complete contact information is available at: https://pubs.acs.org/10.1021/acs.langmuir.0c01168

Author Contributions

G.N., W.R., and Y.H.X. designed the work. H.P.W., L.Y.J., O.L., J.Y.Z., and Y.Y.L. performed the experiments including the L.B. assembly of 2D colloidal crystals, characterizations, and data analysis. H.P.W. and G.N. wrote the manuscript, and all the co-authors discussed the results and revised the manuscript.

Funding

Natural Science Foundation of China (grant no. 51602247). Key R&D Program of Shaanxi Province of China (2020GY-271 and 2018ZDXM-GY-150). The Fundamental Research Funds for the Central Universities (xjj2018016). The "111 Project" of China (B14040). Open Project of State Key Laboratory of Electronic Thin Films and Integrated Devices (KFJJ201902). Open Project of State Key Laboratory of Infrared Technological Physic (M201801).

Notes

The authors declare no competing financial interest.

■ ACKNOWLEDGMENTS

We acknowledge Professor Libo Zhao for his assistance with experiments and Ren at Instrument Analysis Center of Xi'an Jiaotong University for his assistance with SEM analysis.

■ REFERENCES

(1) Aguirre, C. I.; Reguera, E.; Stein, A. Tunable colors in opals and inverse opal photonic crystals. *Adv. Funct. Mater.* **2010**, *20*, 2565−2578.

(2) Chen, K.; Rajeeva, B. B.; Wu, Z.; Rukavina, M.; Dao, T. D.; Ishii, S.; Aono, M.; Nagao, T.; Zheng, Y. Moire Nanosphere Lithography. *ACS Nano* **2015**, *9*, 6031−6040.

(3) Lei, Y.; Yang, S.; Wu, M.; Wilde, G. Surface patterning using templates: concept, properties and device applications. *Chem. Soc. Rev.* **2011**, *40*, 1247−1258.

(4) Henzie, J.; Barton, J. E.; Stender, C. L.; Odom, T. W. Large-area nanoscale patterning: chemistry meets fabrication. *Acc. Chem. Res.* **2006**, *39*, 249−257.

(5) Ye, X.; Qi, L. Two-dimensionally patterned nanostructures based on monolayer colloidal crystals: Controllable fabrication, assembly, and applications. *Nano Today* **2011**, *6*, 608−631.

(6) Wang, Y.; Zhang, M.; Lai, Y.; Chi, L. Advanced colloidal lithography: From patterning to applications. *Nano Today* **2018**, *22*, 36−61.

(7) Rakers, S.; Chi, L. F.; Fuchs, H. Influence of the evaporation rate on the packing order of polydisperse latex monofilms. *Langmuir* **1997**, *13*, 7121−7124.

(8) Jiang, P.; McFarland, M. J. Wafer-scale periodic nanohole arrays templated from two-dimensional nonclose-packed colloidal crystals. *J. Am. Chem. Soc.* **2005**, *127*, 3710−3711.

(9) Jiang, P.; McFarland, M. J. Large-scale fabrication of wafer-size colloidal crystals, macroporous polymers and nanocomposites by spin-coating. *J. Am. Chem. Soc.* **2004**, *126*, 13778−13786.

(10) Dimitrov, A. S.; Nagayama, K. Continuous convective assembling of fine particles into two-dimensional arrays on solid surfaces. *Langmuir* **1996**, *12*, 1303−1311.

(11) Bardosova, M.; Pemble, M. E.; Povey, I. M.; Tredgold, R. H. The Langmuir−Blodgett approach to making colloidal photonic crystals from silica spheres. *Adv. Mater.* **2010**, *22*, 3104−3124.

(12) Rybczynski, J.; Ebels, U.; Giersig, M. Large-scale, 2D arrays of magnetic nanoparticles. *Colloids Surf., A* **2003**, *219*, 1−6.

(13) Oh, J. R.; Moon, J. H.; Yoon, S.; Park, C. R.; Do, Y. R. Fabrication of wafer-scale polystyrene photonic crystal multilayers via the layer-by-layer scooping transfer technique. *J. Mater. Chem.* **2011**, *21*, 14167−14172.

(14) Justo, Y.; Moreels, I.; Lambert, K.; Hens, Z. Langmuir−Blodgett monolayers of colloidal lead chalcogenide quantum dots: morphology and photoluminescence. *Nanotechnology* **2010**, *21*, 295606.

(15) Hur, J.; Won, Y.-Y. Fabrication of high-quality non-close-packed 2D colloid crystals by template-guided Langmuir−Blodgett particle deposition. *Soft Matter* **2008**, *4*, 1261−1269.

(16) Quint, S. B.; Pacholski, C. Extraordinary long range order in self-healing non-close packed 2D arrays. *Soft Matter* **2011**, *7*, 3735−3738.

(17) Li, X.; Gilchrist, J. F. Large-area nanoparticle films by continuous automated Langmuir−Blodgett assembly and deposition. *Langmuir* **2016**, *32*, 1220−1226.

(18) Meng, X.; Qiu, D. Gas-flow-induced reorientation to centimeter-sized two-dimensional colloidal single crystal of polystyrene particle. *Langmuir* **2014**, *30*, 3019−3023.
(19) Portal-Marco, S.; Vallvé, M. À.; Arteaga, O.; Ignés-Mullol, J.; Corbella, C.; Bertran, E. Structure and physical properties of colloidal crystals made of silica particles. *Colloids Surf., A* **2012**, *401*, 38−47.
(20) Park, S.; Lee, H.-B. Effect of pH on monolayer properties of colloidal silica particles at the air/water interface. *Colloid Polym. Sci.* **2012**, *290*, 445−455.
(21) Portal, S.; Vallvé, M. A.; Arteaga, O.; Ignés-Mullol, J.; Canillas, A.; Bertran, E. Optical characterization of colloidal crystals based on dissymmetric metal-coated oxide submicrospheres. *Thin Solid Films* **2008**, *517*, 1053−1057.
(22) Parchine, M.; McGrath, J.; Bardosova, M.; Pemble, M. E. Large Area 2D and 3D Colloidal Photonic Crystals Fabricated by a Roll-to-Roll Langmuir−Blodgett Method. *Langmuir* **2016**, *32*, 5862−5869.
(23) Li, J.; Li, J.; Xia, X. H. Large-Scale and Well-Ordered Assembly of Microspheres in a Small Container. *Langmuir* **2019**, *35*, 8413−8417.
(24) Tanaka, A.; Tsuchiya, Y.; Usami, K.; Saito, S.-i.; Arai, T.; Mizuta, H.; Oda, S. Synthesis of Assembled Nanocrystalline Si Dots Film by the Langmuir−Blodgett Technique. *Jpn. J. Appl. Phys.* **2008**, *47*, 3731.
(25) Reguera, J.; Ponomarev, E.; Geue, T.; Stellacci, F.; Bresme, F.; Moglianetti, M. Contact angle and adsorption energies of nanoparticles at the air-liquid interface determined by neutron reflectivity and molecular dynamics. *Nanoscale* **2015**, *7*, 5665−5673.
(26) Lu, G. W.; Gao, P. Emulsions and Microemulsions for Topical and Transdermal Drug Delivery. *Handbook of Non-Invasive Drug Delivery Systems*; Elsevier, 2010; pp 59−94.
(27) Ramé, E. The Interpretation of Dynamic Contact Angles Measured by the Wilhelmy Plate Method. *J. Colloid Interface Sci.* **1997**, *185*, 245−251.
(28) Moon, G. D.; Lee, T. I.; Kim, B.; Chae, G.; Kim, J.; Kim, S.; Myoung, J.-M.; Jeong, U. Assembled monolayers of hydrophilic particles on water surfaces. *ACS Nano* **2011**, *5*, 8600−8612.
(29) Phan, M. D.; Shin, K. Effects of cardiolipin on membrane morphology: a Langmuir monolayer study. *Biophys. J.* **2015**, *108*, 1977−1986.
(30) Zanini, M.; Isa, L. Particle contact angles at fluid interfaces: pushing the boundary beyond hard uniform spherical colloids. *J. Phys.: Condens. Matter* **2016**, *28*, 313002.
(31) Maestro, A.; Santini, E.; Zabiegaj, D.; Llamas, S.; Ravera, F.; Liggieri, L.; Ortega, F.; Rubio, R. G.; Guzman, E. Particle and Particle-Surfactant Mixtures at Fluid Interfaces: Assembly, Morphology, and Rheological Description. *Adv. Condens. Matter Phys.* **2015**, *2015*, 1−17.
(32) Li, Y.; Pham, J. Q.; Johnston, K. P.; Green, P. F. Contact angle of water on polystyrene thin films: Effects of CO_2 environment and film thickness. *Langmuir* **2007**, *23*, 9785−9793.
(33) Reculusa, S.; Ravaine, S. Synthesis of colloidal crystals of controllable thickness through the Langmuir−Blodgett technique. *Chem. Mater.* **2003**, *15*, 598−605.
(34) Jung, M.-H.; Yun, H.-G.; Kim, S.; Kang, M. G. ZnO nanosphere fabrication using the functionalized polystyrene nanoparticles for dye-sensitized solar cells. *Electrochim. Acta* **2010**, *55*, 6563−6569.
(35) Dijkstra, M. Entropy-driven phase transitions in colloids: From spheres to anisotropic particles. *Adv. Chem. Phys.* **2015**, *156*, 35−71.
(36) Nikolaides, M. G.; Bausch, A. R.; Hsu, M. F.; Dinsmore, A. D.; Brenner, M. P.; Gay, C.; Weitz, D. A. Electric-field-induced capillary attraction between like-charged particles at liquid interfaces. *Nature* **2002**, *420*, 299.
(37) Denkov, N.; Velev, O.; Kralchevski, P.; Ivanov, I.; Yoshimura, H.; Nagayama, K. Mechanism of formation of two-dimensional crystals from latex particles on substrates. *Langmuir* **1992**, *8*, 3183−3190.
(38) Gasser, U. Crystallization in three-and two-dimensional colloidal suspensions. *J. Phys.: Condens. Matter* **2009**, *21*, 203101.
(39) Frenkel, D. Entropy-driven phase transitions. *Physica A* **1999**, *263*, 26−38.
(40) Sirotkin, E.; Apweiler, J. D.; Ogrin, F. Y. Macroscopic ordering of polystyrene carboxylate-modified nanospheres self-assembled at the water−air interface. *Langmuir* **2010**, *26*, 10677−10683.
(41) Binks, B. P. Particles as surfactants—similarities and differences. *Curr. Opin. Colloid Interface Sci.* **2002**, *7*, 21−41.
(42) Chan, D. Y. C.; Henry, J. D., Jr; White, L. R. The interaction of colloidal particles collected at fluid interfaces. *J. Colloid Interface Sci.* **1981**, *79*, 410−418.
(43) Nicolson, M. M. The interaction between floating particles. *Math. Proc. Cambridge.* **1949**, *45*, 288−295.
(44) Gu, Z.-Z.; Fujishima, A.; Sato, O. Patterning of a colloidal crystal film on a modified hydrophilic and hydrophobic surface. *Angew. Chem., Int. Ed.* **2002**, *41*, 2067−2070.
(45) Reculusa, S.; Ravaine, S. Colloidal photonic crystals obtained by the Langmuir−Blodgett technique. *Appl. Surf. Sci.* **2005**, *246*, 409−414.
(46) Reculusa, S.; Massé, P.; Ravaine, S. Three-dimensional colloidal crystals with a well-defined architecture. *J. Colloid Interface Sci.* **2004**, *279*, 471−478.
(47) Zhang, J.; Sun, Z.; Yang, B. Self-assembly of photonic crystals from polymer colloids. *Curr. Opin. Colloid Interface Sci.* **2009**, *14*, 103−114.
(48) Nair, R. V.; Vijaya, R. Photonic crystal sensors: An overview. *Prog. Quant. Electron.* **2010**, *34*, 89−134.
(49) Zhang, J.-T.; Wang, L.; Luo, J.; Tikhonov, A.; Kornienko, N.; Asher, S. A. 2-D array photonic crystal sensing motif. *J. Am. Chem. Soc.* **2011**, *133*, 9152−9155.
(50) Wang, J.; Wen, Y.; Ge, H.; Sun, Z.; Zheng, Y.; Song, Y.; Jiang, L. Simple fabrication of full color colloidal crystal films with tough mechanical strength. *Macromol. Chem. Phys.* **2006**, *207*, 596−604.
(51) Fudouzi, H.; Xia, Y. Photonic papers and inks: color writing with colorless materials. *Adv. Mater.* **2003**, *15*, 892−896.
(52) Zhong, K.; Li, J.; Liu, L.; Van Cleuvenbergen, S.; Song, K.; Clays, K. Instantaneous, simple, and reversible revealing of invisible patterns encrypted in robust hollow sphere colloidal photonic crystals. *Adv. Mater.* **2018**, *30*, 1707246.
(53) Wang, Z.; Guo, Z. Biomimetic superwettable materials with structural colours. *Chem. Commun.* **2017**, *53*, 12990−13011.

https://dx.doi.org/10.1021/acs.langmuir.0c01168
Langmuir 2020, 36, 10061−10068